JACS Au
AN OPEN ACCESS JOURNAL OF THE AMERICAN CHEMICAL SOCIETY

pubs.acs.org/jacsau
Article

Photocontrolled Reversibly Chiral-Ordered Assembly Based on Cucurbituril

Guoxing Liu, Changming Tian, Xinhui Fan, Xiaoping Xue, Li Feng, Conghui Wang, and Yu Liu*

Cite This: JACS Au 2023, 3, 2550−2556
Read Online

ACCESS | Metrics & More | Article Recommendations | Supporting Information

ABSTRACT: Chirality transfer and regulation, accompanied by morphology transformation, arouse widespread interest for application in materials and biological science. Here, a photocontrolled supramolecular chiral switch is fabricated from chiral diphenylalanine (L-Phe-L-Phe, FF) modified with naphthalene (**2**), achiral dithienylethene (DTE) photoswitch (**1**), and cucurbit[8]uril (CB[8]). Chirality transfer from the chiral FF moiety of **2** to a charge-transfer (CT) heterodimer consisting of achiral guest **1** and achiral naphthalene (NP) in **2** has been unprecedented achieved via the encapsulation of CB[8]. On the contrary, chirality transfer from chiral FF to NP cannot be conducted in only guest **2**. Crucially, induced circular dichroism of the heterodimer can be further modulated by distinct light, attributing to reversible photoisomerization of the DTE. Meanwhile, topological nanostructures are changed from one-dimensional (1D) nanofibers to two-dimensional (2D) nanosheets in the orderly assembling process of the heterodimer, which further achieved reversible interconversion between 2D nanosheets and 1D nanorods with tunable-induced chirality stimulated by diverse light.

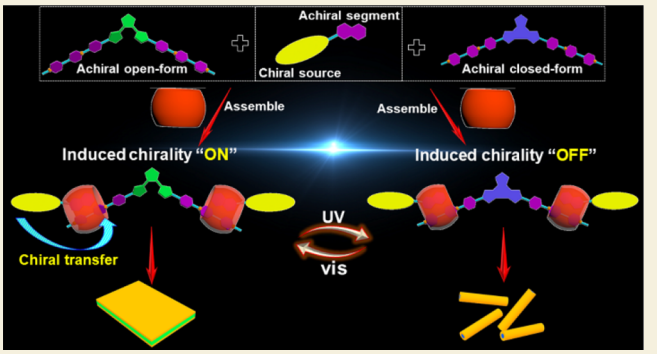

KEYWORDS: *chirality transfer, chirality photoswitch, topological transformation, self-assembly, host-guest complexation*

INTRODUCTION

Chirality exists generally in most of biomolecules and has been intensively studied since Pasteur-resolved tartaric acid.[1] The enantioselective synthesis of chemical compounds is of particular significance for the pharmaceutical field on account of the chiral recognitions between drug and biomolecules.[2] Therefore, chiral transfer (or induction) is very significant and has attracted growing attention.[3−9] A variety of strategies have been applied to chiral transfer (or induction), such as covalent bond,[10] hydrogen bond,[3,11,12] metal coordination,[13] host−guest complexation,[14,15] and so on. Recently, the dynamic control of chirality has progressively become a research hotspot. Various physical and chemical stimuli, such as pH,[16] solvent,[17,18] additive,[19] light,[20−23] redox,[24−27] and heat,[28,29] have been applied to well-organized chiral adjustment. Light is considered as a very favorable candidate for its noninvasiveness, easy controllability, low cost, and ubiquity.[30] Dithienylethenes (DTEs) are one of the most appealing molecules due to their outstanding thermal stability, rapid response, and fatigue resistance in comparison with other photoactive molecules.[31−33] Hecht's group reported a DTE-based photoswitch incorporated by the natural monoterpene L-menthone, and the chirality could be regulated by altering the irradiation conditions or the chemical environment.[34] Zhu and co-workers demonstrated that a helical hydrogen-bonded self-assembly based on DTE-modified chiral naphthalene imide is reversibly switched by distinct light, accompanied by the modulation of morphology, fluorescence, and helicity.[35] On the other hand, controllable transformation of different-dimensional morphologies emerged as an attractive theme in the research of supramolecular chemistry and materials science, because diverse-dimensional nanoaggregates display distinct fascinating functions. Recently, Takeuchi et al. reported one-dimensional/two-dimensional transformation between nanofibers and nanosheets via the controllable kinetic self-assembly process of a metastable porphyrin.[36] Our group developed reversible zero/one-dimensional conversion between nanoparticles and nanotubes, one/two-dimensional transformation between nanofibers and nanosheets, and one/two-dimensional change between nanosheets and nanotubes through stimuli-responsive kinetic assembly.[37−40]

Nevertheless, chirality transfer from a small and simple chiral source to a large and complex achiral charge-transfer (CT) heterodimer mediated by a macrocyclic host with an accompanying different-dimensional morphological change in

Received: June 28, 2023
Revised: August 8, 2023
Accepted: August 8, 2023
Published: August 18, 2023

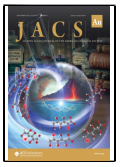

https://doi.org/10.1021/jacsau.3c00342
JACS Au 2023, 3, 2550−2556

an orderly assembling process, which can be further regulated by diverse light, has not been reported yet. Herein, we present a dithienylethene/diphenylalanine/cucurbituril-contained multicomponent supramolecular heterodimer (Scheme 1), which

Scheme 1. Schematic Illustration of the Formation of $1{\cdot}2_2 \subset CB[8]_2$ and Chirality Transfer Photoswitch; Chemical Structures of Assembled Precursors 1, 2, BP, NP, and CB[8]

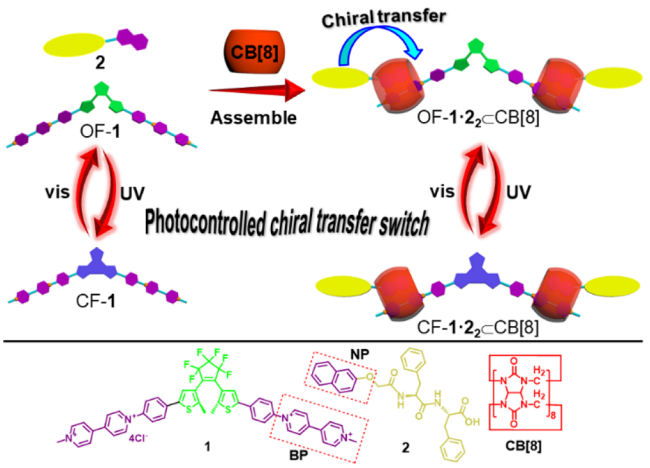

is constructed by photoswitchable DTE-bridged doubly charged bispyridinium (BP) salt (**1**), naphthalene (NP)-substituted chiral diphenylalanine (**2**), and cucurbit[8]uril (CB[8]). The ingenious design is as follows: (1) NP and BP groups are introduced into two guests, respectively, and thus, the two guests can be easily and automatically linked together via encapsulation of rigid CB[8]; (2) diphenylalanine (L-Phe-L-Phe, FF) as a chiral source is introduced into the supramolecular system and provides the possibility of chiral transfer; (3) intermolecular hydrogen-bond interaction of FF and aromatic stacking effect of DTE supply a self-aggregated chance; (4) intervention of DTE endows the supramolecular assembly with optical responsiveness and hopefully achieves photocontrolled chirality transfer switch and orderly topological transformation.

RESULTS

The synthetic routes of guests **1** and **2** are shown in Scheme S1. The photoactive molecular **1** with good water solubility was synthesized via methylation of **3**[41] and subsequent counterion exchange with tetrabutylammonium chloride in 94% yield. Moreover, the reaction of diphenylalanine (L-Phe-L-Phe, FF) **4**[38] with β-naphthol **5** obtained compound **6** in 91% yield, and subsequent hydrolyzation obtained **2** in 88% yield. The chemical structures of these compounds were completely characterized by ^{1}H NMR, ^{13}C NMR, ^{19}F NMR, and HR-MS (see Figures S1–S10).

As expected, compound **1** exhibited excellent reversible photochromic and photoisomerization properties. As shown in Figure S11a, the absorption maximum of the open form of **1** (OF-**1**), which occurred at 275 and 384 nm, declined, and two new absorption peaks at 318 and 615 nm appeared and increased with the generation of three well-defined isosbestic points at 302, 356, and 470 nm upon 254 nm UV light irradiation. The aforementioned observations revealed that photoisomerization of OF-**1** to its closed form (CF-**1**) took place. Moreover, the solution color gradually turned from yellow to blue, implying that the photoreaction was proceeding (Figure S11a, inset). Subsequently, the absorption spectrum and color of the resultant solution thoroughly restored to the original state upon >490 nm visible light irradiation, while the present process above could be repeated for at least seven cycles without any recession, manifesting good fatigue resistance (Figure S11b). The photocyclization quantum yield (Φ_{o-c}) and photo-cycloreversion quantum yield (Φ_{c-o}) of **1** were determined to be 0.09 and 0.002, respectively. Furthermore, the cyclization conversion yield was determined to be approximately 88% by calculating the change of nuclear magnetic integral area (H_g or H_h) with irradiation of 254 nm light (Figure S12), and >500 nm light irradiation led to the recurrence of the original nuclear magnetism (Figure S13), also indicating good photoisomerization reversibility.

After the investigation on photochromic properties of **1**, assembling behaviors of the photosensitive molecule with **2** and CB[8] were further studied. It is well known that the electron-deficient BP unit and electron-rich NP can be jointly encapsulated in the cavity of CB[8] via host–guest interaction to form a 1:1:1 stable CT complex.[42,43] Therefore, 2 equiv of **2**, 1 equiv of **1**, and 2 equiv of CB[8] could self-assemble to be a supramolecular heterodimer $1{\cdot}2_2 \subset CB[8]_2$ in aqueous solution. As depicted in Figure S14, the resonance for BP proton of **1** and NP of **2** all displayed an apparent upfield shift and passivation, implying that BP and NP units were located in the cavity of CB[8] and nanoaggregates formed. To confirm the assembly mode more definitely, we selected NP as the model molecule to replace **2** for avoiding further aggregation. As shown in Figure S15, an apparent upfield shift for the protons of BP in **1** and NP was distinctly observed. In addition, hydrogen–hydrogen correlation for the protons of BP in **1** and NP can be clearly found in the 2D NOESY spectrum (Figure S16). Subsequently, BP instead of **1** was selected to integrate with guest **2** through the encapsulation of CB[8], and their assembling behaviors were investigated. Notably, the proton signals of BP, NP, and one phenyl group of FF in **2** were shifted apparently upfield (Figure S17), indicating that these parts were located in the cavity of CB[8], which is similar to the previous report.[38] In addition, UV–vis absorption and fluorescence emission spectral investigation also provided powerful evidence. As manifested in Figure 1, a new long-wavelength absorption peak at 418 nm different from **1** and **2** was observed in $1{\cdot}2_2 \subset CB[8]_2$ assembly, implying the formation of a stable CT complex. Intuitively, the solution

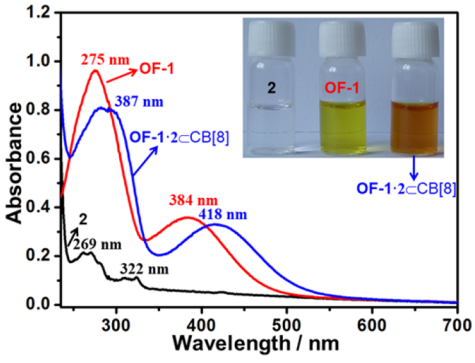

Figure 1. Absorption spectra of **1**, **2**, and heterodimer $1{\cdot}2_2 \subset CB[8]_2$ ($[2] = [CB[8]] = 2[1] = 2 \times 10^{-5}$ M). Inset: color of **1**, **2**, and $1{\cdot}2_2 \subset CB[8]_2$ in aqueous solution ($[2] = [CB[8]] = 2[1] = 4 \times 10^{-5}$ M).

https://doi.org/10.1021/jacsau.3c00342
JACS Au 2023, 3, 2550–2556

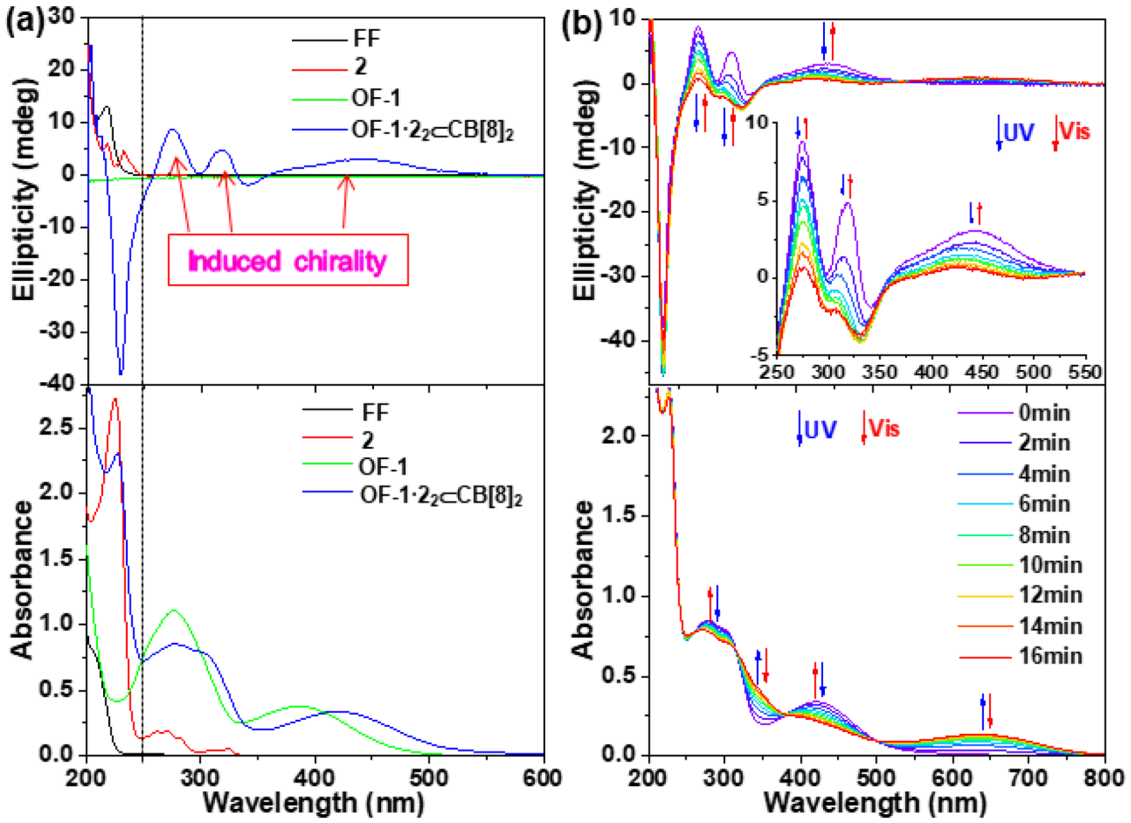

Figure 2. (a) Circular dichroism and UV−vis absorption spectra of OF-**1**, **2**, and OF-**1**·$\mathbf{2}_2$ ⊂ $CB[8]_2$; (b) alteration of circular dichroism and UV−vis absorption spectra of OF-**1**·$\mathbf{2}_2$ ⊂ $CB[8]_2$ upon alternating UV and visible light irradiation; Inset: partial enlargement of panel (b); [**2**] = [CB[8]] = 2[**1**] = 2 × 10^{-4} M; pathlength: 5 mm.

color turned from yellow to orange-red in the mixing process (Figure 1, inset). Moreover, as displayed in Figure S18, **2** emitted at 345 nm, and the mixture composed of 2 equiv of **2**, 1 equiv of **1**, and 2 equiv of CB[8] did not manifest apparent fluorescence emission because of intermolecular CT interaction. Overall, the aforementioned observations convincingly indicated the formation of supramolecular heterodimer **1**·$\mathbf{2}_2$ ⊂ $CB[8]_2$, as displayed in Scheme 1.

The introduction of chiral group FF encouraged us to investigate circular dichroism (CD) spectroscopy of monomer **2** and assembly **1**·$\mathbf{2}_2$ ⊂ $CB[8]_2$. As depicted in Figure 2a, **2** showed obvious CD signals around 225 nm assigned to benzene rings of FF. Furthermore, a strong positive CD band around 200 nm (π−π* transition) was observed, corresponding to the assumed β-turns of FF.[44] However, the NP group of **2** did not manifest an apparent CD signal at 269 and 322 nm, suggesting that no chirality transfer occurred between NP and FF, ascribed to the far distance and flexible linker. Afterward, we also examined the CD spectrum of molecular switch **1** for comparison, which revealed that the open form of **1** (OF-**1**) also showed no CD signals. It is well known that simple CB[8] is an achiral macrocyclic host. Moreover, we performed CD spectroscopy of D-Phe-D-Phe (Figure 2a), which also displayed positive CD signals as guest **2**. Nevertheless, chiral inversion and amplification with a strong negative CD signal (−38 mdeg) at 225 nm that belonged to FF occurred in the formation of **1**·**2** ⊂ $CB[8]_2$. This was probably attributed to the distinct alteration of configuration of FF and formation of a more rigid structure caused by host−guest complexation and hydrogen-bond interaction. To our surprise, apparent CD signals among 250−350 nm (belonging to the NP unit and photochromic molecule **1**) and 350−550 nm (assigned to the CT complex) were observed, indicating that chirality transfer from FF to the CT heterodimer took place in the assembling process.

To further affirm the aforementioned viewpoints, we selected BP, a segment of **1**, as a reference to examine chirality transfer between FF in **2** and CT complex formed by BP and NP in **2**. Then, an investigation of the assembly BP·**2** ⊂ CB[8] was performed using CD spectroscopy. The similar chiral inversion and amplification of assembly BP·**2** ⊂ CB[8] as **1**·$\mathbf{2}_2$ ⊂ $CB[8]_2$ at 228 nm assigned to benzene rings of FF were observed relative to **2** (Figure S19a). Moreover, apparent CD signals between 250 and 335 nm (assigned to NP and BP) were found, while the absorption band of the CT complex at 335−460 nm band displayed positive CD signals because of the formation of inclusion complex BP·**2** ⊂ CB[8] (Figure S19b). On the contrary, there are no apparent CD signals between 225 and 460 nm for compounds BP and **2**, which was consistent with the observation in Figure 2a. The observations above jointly verified that the chirality of CT complex consisting of NP, BP, and CB[8] was induced by FF. Then, we speculated that the causes of the above chirality transfer should be as follows: (1) the formation of supramolecular assemblies BP·**2** ⊂ CB[8] and **1**·$\mathbf{2}_2$ ⊂ CB[8] shortened the distance from chiral sources of FF (chiral donor) to the CT complex (chiral acceptor) through host−guest complexation and hydrogen-bond (H-bond) interaction between the carbonyls of CB[8] and the amino hydrogen atoms of FF; (2) intervention of CB[8] into the system caused the whole

https://doi.org/10.1021/jacsau.3c00342
JACS Au 2023, 3, 2550−2556

molecular configuration of supramolecular assemblies BP·**2** ⊂ CB[8] and **1**·$\mathbf{2}_2$ ⊂ $CB[8]_2$ to become more rigid than the free guest **2**. The corresponding proof came from the 2D ROESY spectra of the **2**·BP ⊂ CB[8] assembly and density functional theory calculation (DFT). The 2D ROESY spectra of the assembly manifested that aryl groups in guest **2** and BP possessed obvious hydrogen−hydrogen correlation with CB[8] (Figure S20). The geometry-optimized structure of the inclusion complex (Figure 3) was determined through density

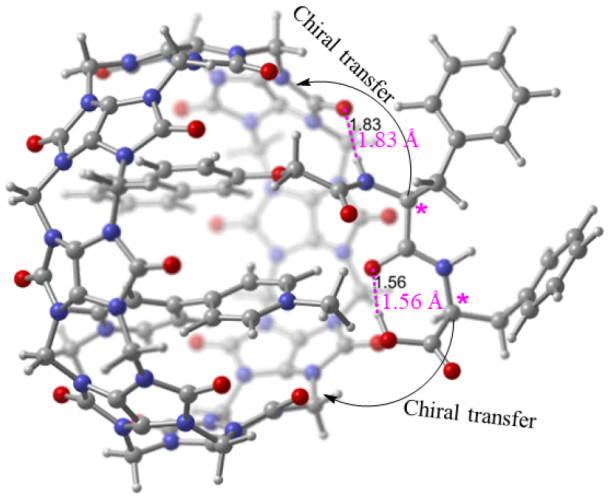

Figure 3. Geometry-optimized structures of host−guest complex BP·**2** ⊂ CB[8] and its chiral transfer mechanism.

functional theory (DFT) calculation, indicating that NPs in **2** and BP were encapsulated in the cavity of CB[8] and a H-bond formed between the amido bond near the naphthalene group in FF and one carbonyl in CB[8] (their distance was 1.83 Å, well within the H-bond range).

More interestingly, when the open form of **1**·$\mathbf{2}_2$ ⊂ $CB[8]_2$ (OF-**1**·$\mathbf{2}_2$ ⊂ $CB[8]_2$) was irradiated by 254 nm wavelength light, the induced CD signals among 250−350 nm (belonging to the NP unit and photosensitive molecule **1**) and 350−550 nm (assigned to the CT complex) faded away, attributed to the conversion from OF-**1**·$\mathbf{2}_2$ ⊂ $CB[8]_2$ to CF-**1**·$\mathbf{2}_2$ ⊂ $CB[8]_2$ (Figure 2b). Subsequently, >600 nm visible light irradiation enabled the absorption and CD spectra to return to the original state states, originating from the regeneration of OF-**1**·$\mathbf{2}_2$ ⊂ $CB[8]_2$ (Figure 2b). The above process could be cycled for five times without any obvious recession (Figure S21), manifesting satisfying fatigue resistance, which was attributed to good photochromic reversibility (Figure S22). In a word, the induced chirality could be reversibly switched "on" and "off" upon alternating UV and visible light irradiation. Furthermore, the CD peak at 225 nm remained almost constant in this irradiation process, because only the DTE part of **1** exhibited reversible isomerization and the parts of FF and CB[8] had changed very little. Interestingly, the solid-state CD spectra of the **1**·$\mathbf{2}_2$ ⊂ $CB[8]_2$ assembly showed alteration upon irradiation at alternating 254 and >600 nm light, indicating that the solid-state assembly still kept switchable chiroptical properties to some extent (Figure S23).

On the other hand, to our delight, tunable morphological alteration was accompanied by the aforementioned orderly self-assembling and irradiation process. The evidence of topological features comes from transmission electron microscopy (TEM) and scanning electron microscopy (SEM). To begin with, **2** in ethanol/water (V/V = 1:19) solution formed many nanofibers with the width of 26 nm, as was observed in TEM (Figure 4a). Additional proof was

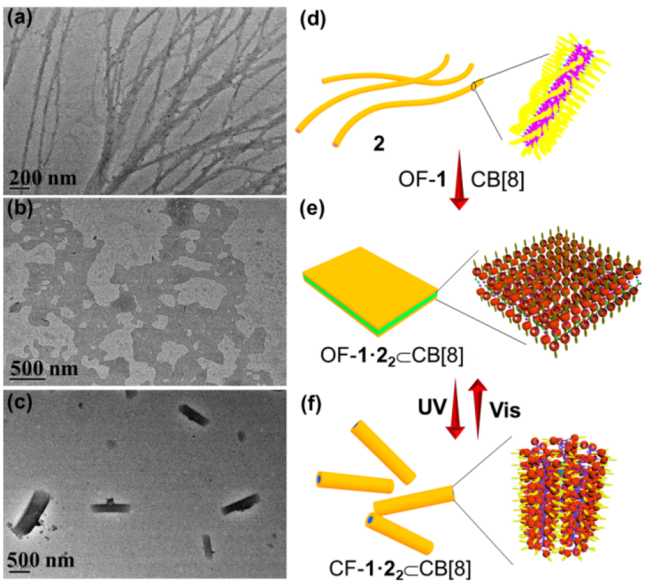

Figure 4. TEM images of **2** (a), OF-**1**·$\mathbf{2}_2$ ⊂ $CB[8]_2$ (b), and CF-**1**·$\mathbf{2}_2$ ⊂ $CB[8]_2$ (c); possible morphological formation mechanisms of **2** (d), OF-**1**·$\mathbf{2}_2$ ⊂ $CB[8]_2$ (e), and CF-**1**·$\mathbf{2}_2$ ⊂ $CB[8]_2$ (f).

supported by SEM (Figure S24a), displaying many nanofibers as well, which is absolutely consistent with TEM. Second, in the orderly assembling process of supramolecular heterodimer **1**·$\mathbf{2}_2$ ⊂ $CB[8]_2$, the one-dimensional (1D) nanofibers were changed to two-dimensional (2D) nanosheets. As discerned in the TEM image (Figure 4b), we could find many 2D nanosheets in our sight, which was further confirmed by SEM (Figure S24b). Meanwhile, the thickness of the layered structure was determined to be approximately 7.8 nm by AFM (Figure S25). In addition, reversible photoisomerization of **1** inspired us to further examine whether the topological morphology was altered. Irradiation at 254 nm wavelength light led to ordered morphology transformation from 2D nanosheets to 1D nanorods because of structural conversion of the **1**·$\mathbf{2}_2$ ⊂ $CB[8]_2$ assembly from open form to closed form. As discerned from Figure 4c, many rodlike nanostructures could be observed in the TEM image, which is basically consistent with the feature displayed in the SEM image (Figure S24c). Crucially, the initial morphology of **1**·$\mathbf{2}_2$ ⊂ $CB[8]_2$ (nanosheets) could be recovered after irradiation at >600 nm visible light, benefiting from reversible photoisomerization of **1**·$\mathbf{2}_2$ ⊂ $CB[8]_2$ (Figure S22). Significantly, topological morphology alteration from 1D nanofibers to 2D nanosheets and then optically controlled reversible interconversion between 2D nanosheets and 1D nanorods along with chiral modulation were realized in the present process.[45]

Finally, we deduced a possible morphological formation and interconversion mechanism, as illustrated in Figure 4d−f. In the self-aggregate of **2**, $\pi-\pi$ stacking arrangements between hydrophobic NP rings as the core of nanofiber and hydrogen bonds between hydrophilic peptide main chains as the outer part promoted the formation of nanofibers (Figure 4d).[46] This is consistent with the previous reports that the short peptides had a major tendency to form long fibers in aqueous

https://doi.org/10.1021/jacsau.3c00342
JACS Au 2023, 3, 2550−2556

solutions.[47] However, the OF-$\mathbf{1{\cdot}2_2}$ ⊂ CB[8]$_2$ assembly possessed two FF in opposite directions, which would grow along two perpendicular directions. This adopts a side-by-side array along the horizontal direction but a head-to-head (or tail) array along the vertical direction, and the resultant 2D structure was stabilized by the hydrogen bonds and $\pi-\pi$ interactions among adjacent OF-$\mathbf{1{\cdot}2_2}$ ⊂ CB[8]$_2$ units (Figure 4e).[48] When the open form of $\mathbf{1{\cdot}2_2}$ ⊂ CB[8]$_2$ was transformed into its closed form, the DTE framework became more rigid and formed $\pi-\pi$ stacking more easily. DTE and accessory aromatic rings as cores and FF as peripheries formed nanofibers and then aggregated to nanorods with larger radius (Figure 4f). In addition, the hydrodynamic radii of the two assemblies OF-$\mathbf{1{\cdot}2_2}$ ⊂ CB[8]$_2$ and CF-$\mathbf{1{\cdot}2_2}$ ⊂ CB[8]$_2$ were determined to be ca. 120 and 350 nm, respectively, by DLS (Figure S26), and such a big distinction further proved an apparent morphological change, which further implied changes in their assembling patterns.

CONCLUSIONS

In summary, a supramolecular heterodimer containing DTE, FF, and CB[8] has been tactfully developed through host–guest complexation. Surprisingly, chirality transfer from FF in guest **2** to the CT heterodimer formed by achiral OF-**1** and achiral NP in **2** was achieved in this assembling process, ascribed to the shortened distance between the chirality donor and acceptor and more rigid structure caused by encapsulation of CB[8] and hydrogen-bond interaction. However, chirality transfer from FF to NP cannot be conducted in only guest **2** because of non-conjugated flexible connection. Interestingly, the induced chirality can be further reversibly modulated by UV and visible light in the presence of photosensitive DTE, and the process can be cycled for at least seven times without obvious fatigue. Furthermore, 1D chiral nanofiber was changed into organic 2D nanosheet with induced chirality in the orderly assembling process, and subsequently, reversible interconversion between organic 2D nanosheet and 1D nanorod with adjustable induced chirality can be realized upon irradiation at distinct light. The present study provides a convenient approach to designing and constructing photosensitive supramolecular aggregates that integrate chirality transfer, chirality switch, and topological morphology conversion.

METHODS

All manipulations were carried out under an argon atmosphere by using standard Schlenk techniques, unless otherwise stated. THF was distilled under an argon atmosphere from sodium-benzophenone. All other starting materials were obtained commercially as analytical grade and used without further purification. All the property examinations were performed at room temperature, unless noted otherwise. The ^{1}H NMR and ^{13}C NMR spectra were recorded on a Bruker AV400 spectrometer at 25 °C. The time-of-flight mass spectra were measured in the MALDI mode. Optical absorption was measured in a quartz cell (pathlength, 10 and 5 mm) on a Shimadzu UV-2401PC spectrophotometer equipped with a Thermo HAAKE-SC100 temperature controller. The steady-state fluorescence spectra were recorded in a conventional quartz cell (light path, 10 mm) on a HITACHI F-7000 FL. The circular dichroism (CD) spectra were measured in a quartz cell (pathlength, 10 and 5 mm) on a JASCO J-715 spectropolarimeter. TEM images were acquired using a Tecnai 20 transmission electron microscope operated at an accelerating voltage of 200 kV. Samples for TEM measurements were prepared by dropping a sample solution (20 μM) onto a copper grid. The grid was then air-dried. SEM images were recorded on a HITACHI S-3500N scanning electron microscope. The UV light irradiation experiment was carried out using a germicidal lamp ZF-7A (254 nm, 8 W), and the visible light irradiation experiments (λ > 490 nm and λ > 600 nm) were carried out using a CEL-HXF300 20 V 300 W xenon lamp (Beijing China Education Au-light Co. Ltd., China) with a 25% attenuating filter and cutoff optical filter for >490 and >600 nm light, respectively.

ASSOCIATED CONTENT

Supporting Information

The Supporting Information is available free of charge at https://pubs.acs.org/doi/10.1021/jacsau.3c00342.

Compound synthesis and characterization and additional figures in the optical experiments (PDF)

AUTHOR INFORMATION

Corresponding Author

Yu Liu − *College of Chemistry, State Key Laboratory of Elemento-Organic Chemistry, Nankai University, Tianjin 300071, P. R. China;* orcid.org/0000-0001-8723-1896; Email: yuliu@nankai.edu.cn

Authors

Guoxing Liu − *College of Chemistry, State Key Laboratory of Elemento-Organic Chemistry, Nankai University, Tianjin 300071, P. R. China; College of Science, Henan Agricultural University, Zhengzhou, Henan 450002, P. R. China;* orcid.org/0000-0003-1609-3865

Changming Tian − *College of Science, Henan Agricultural University, Zhengzhou, Henan 450002, P. R. China*

Xinhui Fan − *College of Science, Henan Agricultural University, Zhengzhou, Henan 450002, P. R. China*

Xiaoping Xue − *College of Science, Henan Agricultural University, Zhengzhou, Henan 450002, P. R. China*

Li Feng − *College of Chemistry, State Key Laboratory of Elemento-Organic Chemistry, Nankai University, Tianjin 300071, P. R. China*

Conghui Wang − *College of Chemistry, State Key Laboratory of Elemento-Organic Chemistry, Nankai University, Tianjin 300071, P. R. China*

Complete contact information is available at: https://pubs.acs.org/10.1021/jacsau.3c00342

Author Contributions

CRediT: **Guoxing Liu** investigation, methodology, writing-original draft; **Changming Tian** investigation; **Xinhui Fan** investigation; **Xiaoping Xue** methodology; **Li Feng** formal analysis; **Conghui Wang** formal analysis, investigation; **Yu Liu** supervision, writing-review & editing.

Notes

The authors declare no competing financial interest.

ACKNOWLEDGMENTS

We thank the National Natural Science Foundation of China (nos. 22131008 and 21801063) and Top-Notch Talents Program of Henan Agricultural University (no. 30501049) for financial support.

REFERENCES

(1) Pasteur, L. *Recherches sur les relations qui peuvent exister entre la forme crystalline, la composition chimique et le sens de la polarization rotatoire.* 1848, *24*, 442–459.

(2) Wang, Y.; Xu, J.; Wang, Y.; Chen, H. Emerging chirality in nanoscience. *Chem. Soc. Rev.* **2013**, *42*, 2930−2962.
(3) Deng, M.; Zhang, L.; Jiang, Y.; Liu, M. Role of Achiral Nucleobases in Multicomponent Chiral Self-Assembly: Purine-Triggered Helix and Chirality Transfer. *Angew. Chem., Int. Ed.* **2016**, *55*, 15062−15066.
(4) Goubert, G.; Dong, Y.; Groves, M. N.; Lemay, J.-C.; Hammer, B.; McBreen, P. H. Monitoring interconversion between stereochemical states in single chirality-transfer complexes on a platinum surface. *Nat. Chem.* **2017**, *9*, 531−536.
(5) Masini, F.; Kalashnyk, N.; Knudsen, M. M.; Cramer, J. R.; Lægsgaard, E.; Besenbacher, F.; Gothelf, K. V.; Linderoth, T. R. Chiral Induction by Seeding Surface Assemblies of Chiral Switches. *J. Am. Chem. Soc.* **2011**, *133*, 13910−13913.
(6) Zhang, Y.; Qin, X.; Zhu, X.; Liu, M.; Guo, Y.; Zhang, Z. Direct observation of long-range chirality transfer in a self-assembled supramolecular monolayer at interface in situ. *Nat. Commun.* **2022**, *13*, 7737.
(7) Wang, X.; Wang, Y.; Yang, H.; Fang, H.; Chen, R.; Sun, Y.; Zheng, N.; Tan, K.; Lu, X.; Tian, Z.; Cao, X. Assembled molecular face-rotating polyhedra to transfer chirality from two to three dimensions. *Nat. Commun.* **2016**, *7*, 12469.
(8) Yang, D.; Duan, P.; Zhang, L.; Liu, M. Chirality and energy transfer amplified circularly polarized luminescence in composite nanohelix. *Nat. Commun.* **2017**, *8*, 15727.
(9) Cai, S.; Chen, J.; Wang, S.; Zhang, J.; Wan, X. Allostery-Mimicking Self-assembly of Helical Poly(phenylacetylene) Block Copolymers and the Chirality Transfer. *Angew. Chem., Int. Ed.* **2021**, *60*, 9686−9692.
(10) Campolo, D.; Gastaldi, S.; Roussel, C.; Bertrand, M. P.; Nechab, M. Axial-to-central chirality transfer in cyclization processes. *Chem. Soc. Rev.* **2013**, *42*, 8434−8466.
(11) van Dijken, D. J.; Beierle, J. M.; Stuart, M. C. A.; Szymański, W.; Browne, W. R.; Feringa, B. L. Autoamplification of Molecular Chirality through the Induction of Supramolecular Chirality. *Am. Ethnol.* **2014**, *53*, 5073−5077.
(12) Zhang, Q.; Crespi, S.; Toyoda, R.; Costil, R.; Browne, W. R.; Qu, D.-H.; Tian, H.; Feringa, B. L. Stereodivergent Chirality Transfer by Noncovalent Control of Disulfide Bonds. *J. Am. Chem. Soc.* **2022**, *144*, 4376−4382.
(13) Greenfield, J. L.; Evans, E. W.; Nuzzo, D. D.; Antonio, M. D.; Friend, R. H.; Nitschke, J. R. Unraveling Mechanisms of Chiral Induction in Double-Helical Metallopolymers. *J. Am. Chem. Soc.* **2018**, *140*, 10344−10353.
(14) Yang, C.; Inoue, Y. Supramolecular photochirogenesis. *Chem. Soc. Rev.* **2014**, *43*, 4123−4143.
(15) Fu, H.-G.; Zhang, H.-Y.; Zhang, H.-Y.; Liu, Y. Photo-controlled chirality transfer and FRET effects based on pseudo[3]rotaxane. *Chem. Commun.* **2019**, *55*, 13462−13465.
(16) Lin, R.; Zhang, H.; Li, S.; Chen, L.; Zhang, W.; Wen, T. B.; Zhang, H.; Xia, H. pH-Switchable Inversion of the Metal-Centered Chirality of Metallabenzenes: Opposite Stereodynamics in Reactions of Ruthenabenzene with L- and D-Cysteine. *Chem. − Eur. J.* **2011**, *17*, 2420−2427.
(17) Martinez, A.; Guy, L.; Dutasta, J.-P. Reversible, Solvent-Induced Chirality Switch in Atrane Structure: Control of the Unidirectional Motion of the Molecular Propeller. *J. Am. Chem. Soc.* **2010**, *132*, 16733−16734.
(18) Borovkov, V. V.; Hembury, G. A.; Inoue, Y. The Origin of Solvent-Controlled Supramolecular Chirality Switching in a Bis(Zinc Porphyrin) System. *Angew. Chem., Int. Ed.* **2003**, *42*, 5310−5314.
(19) Qiu, Y.; Chen, P.; Guo, P.; Li, Y.; Liu, M. Supramolecular Chiroptical Switches Based on Achiral Molecules. *Adv. Mater.* **2008**, *20*, 2908−2913.
(20) de Jong, J. J. D.; Lucas, L. N.; Kellogg, R. M.; van Esch, J. H.; Feringa, B. L. Reversible Optical Transcription of Supramolecular Chirality into Molecular Chirality. *Science* **2004**, *304*, 278−281.
(21) Zheng, Z.; Li, Y.; Bisoyi, H. K.; Wang, L.; Bunning, T. J.; Li, Q. Three-dimensional control of the helical axis of a chiral nematic liquid crystal by light. *Nature* **2016**, *531*, 352−356.
(22) Hao, T.; Yang, Y.; Liang, W.; Fan, C.; Wang, X.; Wu, W.; Chen, X.; Fu, H.; Chen, H.; Yang, C. Trace mild acid-catalysed Z→E isomerization of norbornene-fused stilbene derivatives: intelligent chiral molecular photoswitches with controllable self-recovery. *Chem. Sci.* **2021**, *12*, 2614−2622.
(23) Li, M.; Chen, L.-J.; Cai, Y.; Luo, Q.; Li, W.; Yang, H.-B.; Tian, H.; Zhu, W.-H. Light-Driven Chiral Switching of Supramolecular Metallacycles with Photoreversibility. *Chem* **2019**, *5*, 634−648.
(24) Canary, J. W. Redox-triggered chiroptical molecular switches. *Chem. Soc. Rev.* **2009**, *38*, 747−756.
(25) Zhang, Y. J.; Oka, T.; Suzuki, R.; Ye, J. T.; Iwasa, Y. Electrically Switchable Chiral Light-Emitting Transistor. *Science* **2014**, *344*, 725−728.
(26) Ohta, E.; Sato, H.; Ando, S.; Kosaka, A.; Fukushima, T.; Hashizume, D.; Yamasaki, M.; Hasegawa, K.; Muraoka, A.; Ushiyama, H.; Yamashita, K.; Aida, T. Redox-responsive molecular helices with highly condensed π-clouds. *Nat. Chem.* **2011**, *3*, 68−73.
(27) Xiao, C.; Wu, W.; Liang, W.; Zhou, D.; Kanagaraj, K.; Cheng, G.; Su, D.; Zhong, Z.; Chruma, J. J.; Yang, C. Redox-Triggered Chirality Switching and Guest-Capture/Release with a Pillar[6]arene-Based Molecular Universal Joint. *Angew. Chem., Int. Ed.* **2020**, *59*, 8094−8098.
(28) Ooi, T. Heat and Light Switch a Chiral Catalyst and Its Products. *Science* **2011**, *331*, 1395−1396.
(29) Yao, J.; Wu, W.; Liang, W.; Feng, Y.; Zhou, D.; Chruma, J. J.; Fukuhara, G.; Mori, T.; Inoue, Y.; Yang, C. Temperature-Driven Planar Chirality Switching of a Pillar[5]arene-Based Molecular Universal Joint. *Angew. Chem., Int. Ed.* **2017**, *56*, 6869−6873.
(30) Chen, M.; Zhong, M.; Johnson, J. A. Light-Controlled Radical Polymerization: Mechanisms, Methods, and Applications. *Chem. Rev.* **2016**, *116*, 10167−10211.
(31) Irie, M.; Fukaminato, T.; Matsuda, K.; Kobatake, S. Photochromism of Diarylethene Molecules and Crystals: Memories, Switches, and Actuators. *Chem. Rev.* **2014**, *114*, 12174−12277.
(32) Qu, D.-H.; Wang, Q.-C.; Zhang, Q.-W.; Ma, X.; Tian, H. Photoresponsive Host−Guest Functional Systems. *Chem. Rev.* **2015**, *115*, 7543−7588.
(33) Liu, G.; Zhu, J.; Zhou, Y.; Dong, Z.; Xu, X.; Mao, P. Adjustable Photochromic Behavior of a Diarylethene-Based Bistable [3]-Rotaxane. *Org. Lett.* **2018**, *20*, 5626−5630.
(34) Jurissek, C.; Berger, F.; Eisenreich, F.; Kathan, M.; Hecht, S. External Reversal of Chirality Transfer in Photoswitches. *Agnew. Chem., Int. Ed.* **2019**, *58*, 1945−1949.
(35) Cai, Y.; Guo, Z.; Chen, J.; Li, W.; Zhong, L.; Gao, Y.; Jiang, L.; Chi, L.; Tian, H.; Zhu, W.-H. Enabling Light Work in Helical Self-Assembly for Dynamic Amplification of Chirality with Photoreversibility. *J. Am. Chem. Soc.* **2016**, *138*, 2219−2224.
(36) Fukui, T.; Kawai, S.; Fujinuma, S.; Matsushita, Y.; Yasuda, T.; Sakurai, T.; Seki, S.; Takeuchi, M.; Sugiyasu, K. Control over differentiation of a metastable supramolecular assembly in one and two dimensions. *Nat. Chem.* **2017**, *9*, 493−499.
(37) Sun, H.-L.; Chen, Y.; Zhao, J.; Liu, Y. Photocontrolled Reversible Conversion of Nanotube and Nanoparticle Mediated by β-Cyclodextrin Dimers. *Angew. Chem., Int. Ed.* **2015**, *54*, 9376−9380.
(38) Zhang, W.; Zhang, Y.-M.; Li, S.-H.; Cui, Y.-L.; Yu, J.; Liu, Y. Tunable Nanosupramolecular Aggregates Mediated by Host−Guest Complexation. *Angew. Chem., Int. Ed.* **2016**, *55*, 11452−11456.
(39) Sun, H.-L.; Chen, Y.; Han, X.; Liu, Y. Tunable Supramolecular Assembly and Photoswitchable Conversion of Cyclodextrin/Diphenylalanine-Based 1D and 2D Nanostructures. *Angew. Chem., Int. Ed.* **2017**, *56*, 7062−7065.
(40) Zhang, Y.-M.; Zhang, N.-Y.; Xiao, K.; Yu, Q.; Liu, Y. Photo-Controlled Reversible Microtubule Assembly Mediated by Paclitaxel-Modified Cyclodextrin. *Angew. Chem., Int. Ed.* **2018**, *57*, 8649−8653.
(41) Liu, G.; Zhang, Y.-M.; Xu, X.; Zhang, L.; Liu, Y. Optically Switchable Luminescent Hydrogel by Synergistically Intercalating

https://doi.org/10.1021/jacsau.3c00342
JACS Au 2023, 3, 2550−2556

Photochromic Molecular Rotor into Inorganic Clay. *Adv. Opt. Mater.* **2017**, *5*, 1700149.
(42) Kim, K.; Kim, D.; Lee, J. W.; Ko, Y. H.; Kim, K. Growth of poly(pseudorotaxane) on gold using host-stabilized charge-transfer interaction. *Chem. Commun.* **2004**, *848-849*, 848.
(43) Barrow, S. J.; Barrow, S.; Rowland, M. J.; del Barrio, J.; Scherman, O. A. Cucurbituril-Based Molecular Recognition. *Chem. Rev.* **2015**, *115*, 12320−12406.
(44) Gupta, M.; Bagaria, A.; Mishra, A.; Mathur, P.; Basu, A.; Ramakumar, S.; Chauhan, V. S. Self-Assembly of a Dipeptide-Containing Conformationally Restricted Dehydrophenylalanine Residue to Form Ordered Nanotubes. *Adv. Mater.* **2007**, *19*, 858−861.
(45) Sun, S.; Li, X.; Xu, C.; Li, Y.; Wu, Y.; Feringa, B. L.; Tian, H.; Ma, X. Scale effect of circularly polarized luminescent signal of matter. *Natl. Sci. Rev.* **2023**, *10*, nwad072.
(46) Görbitz, C. H. The structure of nanotubes formed by diphenylalanine, the core recognition motif of Alzheimer's β-amyloid polypeptide. *Chem. Commun.* **2006**, *22*, 2332−2334.
(47) Huang, R.; Su, R.; Qi, W.; Zhao, J.; He, Z. Hierarchical, interface-induced self-assembly of diphenylalanine: formation of peptide nanofibers and microvesicles. *Nanotechnology* **2011**, *22*, No. 245609.
(48) Cheng, N.; Chen, Y.; Yu, J.; Li, J.; Liu, Y. Photocontrolled Coumarin-diphenylalanine/Cyclodextrin CrossLinking of 1D Nanofibers to 2D Thin Films. *ACS Appl. Mater. Interfaces* **2018**, *10*, 6810−6814.

https://doi.org/10.1021/jacsau.3c00342
JACS Au 2023, 3, 2550−2556